

Bayesian Analysis of High Dimensional Vector Error Correction Model

Parley R Yang* and Alexander Y Shestopaloff†

This version: 29th December 2023

Abstract

Vector Error Correction Model (VECM) is a classic method to analyse cointegration relationships amongst multivariate non-stationary time series. In this paper, we focus on high dimensional setting and seek for sample-size-efficient methodology to determine the level of cointegration. Our investigation centres at a Bayesian approach to analyse the cointegration matrix, henceforth determining the cointegration rank. We design two algorithms and implement them on simulated examples, yielding promising results particularly when dealing with high number of variables and relatively low number of observations. Furthermore, we extend this methodology to empirically investigate the constituents of the S&P 500 index, where low-volatility portfolios can be found during both in-sample training and out-of-sample testing periods.

arXiv:2312.17061v1 [stat.ME] 28 Dec 2023

*University of Cambridge, United Kingdom

†Queen Mary University of London, United Kingdom and Memorial University of Newfoundland, Canada

Contents

1	Introduction	3
1.1	VECM and a motivation for High Dimensional VECM	3
1.2	Literature Review	3
1.3	Organisation	4
2	Methodology	5
2.1	Hierarchical Bayes Modelling of SSL on VECM	5
2.2	Asymptotic Analysis	5
2.3	Algorithms	7
3	Simulation	10
3.1	Outline of Simulated Examples	10
3.2	Summary of Results	10
4	Empirical application to stable portfolio	14
4.1	Portfolio construction	14
4.2	Data and Preparation	14
4.3	Main Results	14
5	Conclusion	16
5.1	Discussions	16
5.2	Contribution	18
A	Technical appendix	19
A.1	Data processing	19

1 Introduction

Let Y denote a p -dimensional multivariate time series, with $Y_t \in \mathbb{R}^p$ being observed at time $t \in [T]$, and $Y_{t,j} \in \mathbb{R}$ denoting observation of j -th variable at time t . We write $Y(\cdot, j)$ to denote the j -th variable of vector Y , which is a univariate time series. Stationarity of $Y(\cdot, j)$ is considered as the second-order stationarity. Precisely, we say $Y(\cdot, j)$ is stationary if the first moment being finite and independent of time and that the auto-covariance function being finite and independent of time. We denote $Y(\cdot, j) \sim I(0)$ in this scenario. When $Y(\cdot, j) \sim I(0)$ for all $j \in [p]$, we write $Y \sim I(0)$. When $Y(\cdot, j)$ is non-stationary but when $\Delta Y(\cdot, j)$ defined by $\Delta Y(t, j) := Y(t, j) - Y(t-1, j)$ is stationary, we write $Y(\cdot, j) \sim I(1)$. Particularly, when $Y(\cdot, j) \sim I(1)$ for all $j \in [p]$, we write $Y \sim I(1)$.

In this paper, we focus on non-stationary time series $Y \sim I(1)$ and centre the investigation on a Bayesian method to analyse Vector Error Correction Model (VECM), which contains a low-rank matrix $\Pi \in \mathbb{R}^{p \times p}$, $\text{rank}(\Pi) = r$ that lead to linearly independent cointegration relationships, represented by cointegration vectors β_1, \dots, β_r such that $\beta_j Y(\cdot, j) \sim I(0)$. We employ Bayesian modelling on the potentially-sparse Π and further the Bayesian inference on such method of estimations. Two algorithms are designed and run on simulated examples, which produce good results under high p and relatively low T . We further this methodology to empirically study the constituents of S&P 500 index, and found low-volatility portfolios in both in-sample training and out-of-sample testing periods.

1.1 VECM and a motivation for High Dimensional VECM

VECM was first proposed by Engle and Granger (1987), followed by sequential Johansen tests (Johansen 1991) on determining the number of cointegration vector. The general form of VECM takes the form of

$$\Delta Y_t = \Pi Y_{t-1} + f(X_t) + \varepsilon_t, \quad \varepsilon_t \sim N(0, \Sigma) \text{ iid} \quad (1)$$

where $X \sim I(0)$, $Y \sim I(1)$ and f is linear. $\Pi \in \mathbb{R}^{p \times p}$ is known as the cointegration matrix. In this paper, we focus on the VAR(1) part of the VECM, which dismisses the X part of the Equation 1. Precisely, we investigate ¹

$$\Delta Y_t = \Pi Y_{t-1} + \varepsilon_t, \quad \varepsilon_t \sim N(0, \Sigma) \text{ iid}, \text{rank}(\Pi) = r \in \{0, 1, \dots, p-1\} \quad (2)$$

The idea of high dimensional VECM falls in the trendy literature surrounding ‘big data’, in which we have a large amount of variables of interest (p) and a substantial amount of observations taken over time (T). In a traditional statistical setting, we require more observations than unknown parameters — in the setting of Equation 2 we need $T > p^2 + \frac{p(p+1)}{2}$. However, that often means we need a greater amount of observations than the data actually have, in order to estimate the equation. This is particularly concerning in light of change-points or other potential changes of the data over time, which naturally constrains the T available. High dimensional VECM is therefore motivated in the regime where p, T are large but $T \leq p^2$. Certainly, for estimating the non-sparse coordinates of the matrix Π , it is reasonable to impose a feasibility assumption where $T > pr$.

A relevant example that further motivates high dimensional VECM goes as follows. Consider p number of stocks in an asset allocation exercise, i.e. let Y_t be a p -dimensional vector of stock price at time t , encompassing p number of stocks. It is common to assume $Y \sim I(1)$. Then, if we find a non-zero vector $\beta \in \mathbb{R}^{1 \times p}$ such that $\beta Y \sim I(0)$, we have $\mathbb{E}[\beta Y_0] = \mathbb{E}[\beta Y_t] \forall t$. This has profound implications in the portfolio construction, as β would be considered as a stable portfolio, i.e. the value of which is expected to be unchanged over time. We further investigate this empirically in section 4.

1.2 Literature Review

As to literature review, we first review on the method proposed by Liang and Schienle (2019) for Partial Least Squares (PLS), then proceeds into the literature of Spike-and-Slab Lasso (SSL), which was first introduced by Rockova (2018), and subsequently extended in Rockova and George (2018).

Write $A_t := \Delta Y_t := Y_t - Y_{t-1}$ and $B_t := Y_{t-1}$ and let $A, B \in \mathbb{R}^{p \times T}$ be constructed by $A = [A_1, \dots, A_T]$ and $B = [B_1, \dots, B_T]$. The PLS estimation of $\tilde{\Pi}$ proposed by Liang and Schienle (2019)

¹The extra terms may often be handled by Partial Least Squares projection, which then reduce the estimation equation back to the VAR(1) form which we focus on.

takes the form of

$$\tilde{\Pi} = (AB^\top)(BB^\top)^{-1} \quad (3)$$

A QR decomposition is then proposed, taking the form of

$$\tilde{\Pi} = (AB^\top)(BB^\top)^{-1} \quad (4)$$

where $\tilde{R} \in UT(p)$ and $\tilde{S} \in \mathbb{R}^{p \times p}$ is orthogonal. Consequentially $\tilde{\Pi} = \tilde{R}^\top \tilde{S}^\top$ where \tilde{R}^\top is a lower triangular matrix. Liang and Schienle (2019) proceed with group-lasso regression, however, we opted for a different route to investigate the true rank of Π .

The SSL literature mainly concerns scalar response multivariate-regression, i.e. the type taking the form of $y_i = x_i^\top \beta + \varepsilon_i$ for each index i , with x_i and β being p -dimensional vectors and y_i being an one-dimensional observation, while ε_i is an iid draw from a Gaussian distribution with zero mean and unknown variance. β_0 is denoted as the true value of the β parameter. SSL can be thought of as a mixing distribution being imposed on the parameter β , conditional on certain hierarchical Bayes parameters γ , which is then conditionally Bernoulli based on θ , which denotes prior expected fraction of non-zero entries of the true β_0 . A posterior mode estimator then aims to maximise the posterior distribution $\pi(\beta|\theta)$. Write $\hat{\beta} = \operatorname{argmax} \pi(\beta|\theta)$. In Rockova and George (2016), a Beta distribution on θ was proposed to enable further inference on the distribution of the estimator conditional on θ , denoted $\pi(\hat{\beta}|\theta)$, and thereafter the conditional expectation $\mathbb{E}[\theta|\hat{\beta}]$. In Rockova and George (2018), further analyses were drawn on the asymptotic behaviour of $\hat{\beta}$ such as bounding the limiting probability of $\sup_{\beta_0} \mathbb{E}_{\beta_0} \left[\mathbb{P}[\hat{\beta} : \|\hat{\beta} - \beta_0\|_1 > \varepsilon] \right]$ with ε depending on the number of observation n and features dimension p .

In our study, we alter the formation of SSL distribution into a row-wise sparsity identification framework towards a $p \times p$ dimensional matrix which is believed to be potentially sparse. This alteration enables further inference and algorithmic interaction towards the rank of Π , which is the order of cointegration. Such alteration may still be studied asymptotically, as we further the asymptotic investigation into statements on the expected probabilities of $\hat{r} = r$, i.e. the event where we correctly estimate the rank.

1.3 Organisation

The rest of this paper is as follows. Section 2 gives details on SSL distribution on a decomposed VECM, followed by the associated asymptotic analysis and algorithmic design. Section 3 then reports simulated examples under various sample size (T) and features dimension (p), followed by empirical application to stable portfolio in section 4.

2 Methodology

2.1 Hierarchical Bayes Modelling of SSL on VECM

Definition 1 (SSL distribution)

Let $X \in \mathbb{R}$ be a random variable. A Spike-and-Slab Lasso (SSL) prior on X is defined as

$$\pi(X|\gamma) := (1 - \gamma)\psi_0(X) + \gamma\psi_1(X), \quad \gamma \in [0, 1] \quad (5)$$

$$\psi_j(x) := \frac{\lambda_j}{2} \exp(-\lambda_j|x|) \quad \forall j \in \{0, 1\} \text{ with } \lambda_0 > \lambda_1 > 0 \quad (6)$$

We write $X|\gamma \sim SSL(\gamma, \lambda_0, \lambda_1)$

We may interpret $X|\gamma$ as a mixture of two Laplace distribution, with ψ_0 being spiky at around 0 and ψ_1 less spiky.

Recall the [Equation 3](#) and [Equation 4](#) composition of the pre-estimate of Π . Here, we attribute the following definition of SSL distribution on the decomposed VECM. We use the notation $A_t := \Delta Y_t$ and $B_t := \tilde{S}^T Y_{t-1}$ and centralise them into \tilde{A}_t, \tilde{B}_t respectively (see [subsection A.1](#) for granular details of data processing).

Definition 2 (SSL distribution on decomposed VECM)

Let $\tilde{A}_t, \tilde{B}_t \in \mathbb{R}^p$ for all $t \in [T]$, and define $e_t : UT(p) \rightarrow \mathbb{R}^p$ by $e_t(R) = \tilde{A}_t - R^\top \tilde{B}_t$ for all t . An SSL distribution on decomposed VECM takes the form of

$$\tilde{A}_t | \tilde{B}_t, R, \sigma^2 \sim N(R^\top \tilde{B}_t, \sigma^2 I_p), \quad \pi(\sigma^2) \propto \sigma^{-2} \quad \forall t \in [T] \quad (7)$$

$$R(\cdot, j) | \gamma_j \sim SSL(\gamma_j, \lambda_{0,j}, \lambda_1) \quad \forall j \in [p] \quad (8)$$

$$\gamma_j | \theta_j \sim \text{Bernoulli}(\theta_j) \quad \forall j \in [p] \quad (9)$$

$$\theta_j \sim \mathcal{B}(a_j, b_j) \quad \forall j \in [p] \quad (10)$$

Under this setting, we have the Bayes Estimator

$$(\hat{R}^{BE}, \hat{\sigma}^{BE}) = \underset{R \in UT(p), \sigma \in \mathbb{R}_{>0}}{\operatorname{argmin}} \sum_{t \in [T]} \frac{\|e_t(R)\|_2^2}{2\sigma^2} + (n+2) \log(\sigma) + \operatorname{pen}(R, \hat{\theta}^{BE}) \quad (11)$$

$$\hat{\theta}_{i,j}^{BE} = \mathbb{E}[\theta_j | \hat{R}^{BE}(\setminus i, j)] := \int_{[0,1]} \theta_j p(\theta_j | \hat{R}^{BE}([p] \setminus \{i\}, j)) d\theta_j \quad (12)$$

The first two terms of [Equation 11](#) are due to Gaussian assumption ([Equation 7](#)) with Jeffery prior on the variance. The penalty term $\operatorname{pen}(R)$ is due to the SSL assumption ([Equation 8](#)). In particular,

$$\operatorname{pen}(R, \theta) = \sum_{j \in [p]} \left(\lambda_1 \|R(\cdot, j)\|_1 - \sum_{i \in [p]} \log \left(\frac{p_j^*(0, \theta_{i,j})}{p_j^*(R(i, j), \theta_{i,j})} \right) \right) \quad (13)$$

where

$$p_j^*(x, \theta_{i,j}) = \frac{\theta_{i,j} \psi_{1,j}(x)}{\theta_{i,j} \psi_{1,j}(x) + (1 - \theta_{i,j}) \psi_{0,j}(x)} \quad (14)$$

However, practically, as suggested by literature (Rockova and George [2018](#) and Bai, Rockova, and George [2021](#) for instance), the term $\hat{\theta}_{i,j}^{BE}$ may be approximated by

$$\hat{\theta}_j^{ABE} := \int_{[0,1]} \theta_j p(\theta_j | \hat{R}^{BE}(\cdot, j)) d\theta_j \quad (15)$$

for all i . We therefore interact with $\hat{\theta}_j^{ABE}$ instead.

2.2 Asymptotic Analysis

Write $\beta = R^\top$. The idea of asymptotic analysis is to provide probabilistic inference towards the limiting behaviour of estimation matrix \hat{R}^{BE} (equivalently thereafter $\hat{\beta}$) and the rank \hat{r} . In what follows, we introduce some approximate notions of $\hat{\beta}$ and the associated ranks to enable the adaption towards some existing theories and our proposed asymptotic statements.

Definition 3 (Intersection line, generalised dimensionality and rank)

Let $\delta_i := \frac{\log((\hat{p}_i^*(0))^{-1}-1)}{\lambda_{0,i}-\lambda_1}$. This is known as the intersection line.

We construct matrix $\tilde{\beta}$ entry-by-entry as follows:

$$\forall i, j, \quad \tilde{\beta}_{i,j} = \begin{cases} \beta_{i,j} & \text{if } |\beta_{i,j}| > \delta_i \\ 0 & \text{else} \end{cases}$$

We define the generalised dimensionality of row $\tilde{\beta}_i := \tilde{\beta}(i, \cdot)$ and the matrix as

$$\gamma_i(\beta) = \|\tilde{\beta}_i\|_0, \quad \gamma(\beta) = \sum_{i \in [p]} \gamma_i(\beta) \quad (16)$$

We also define the generalised rank $\tilde{r}(\beta_i) := |\{i \in [p] : \gamma_i(\beta) > 0\}|$

As a notational remark, note that for any estimate $\hat{\beta}$, we have the associate notions of $\tilde{\beta}(\hat{\beta}), \gamma_i(\hat{\beta}), \gamma(\hat{\beta}), \tilde{r}(\hat{\beta})$. For the true β , we write $q = \|\beta\|_0 = \gamma(\beta)$. Let r be the rank of the true β .

Assumption 4 (Asymptotic assumptions)

The following asymptotic assumptions are required for Lemma 5 and Theorem 6: there exists $a, b \geq 2$ where $\frac{1-\theta}{\theta} \sim p^a$ and $\lambda_{0,i} \gtrsim p^b \forall i$. λ_1 satisfies $\lambda_1 \in [\frac{\sqrt{T}}{p}, 4\sqrt{T \log p}]$

Below, we briefly outline the posterior concentration from Rockova and George (2018), which leads to the proof of Theorem 6.

Lemma 5 (Posterior concentration under Rockova and George (2018))

There exists M independent of p, K not increasing with p such that as $p, T \rightarrow \infty$,

$$\forall i, \quad \sup_{\beta_i} \mathbb{E}_{\beta_i} \left[\mathbb{P}_{\cdot|D,\theta} \left(\hat{\beta}_i : \|\beta_i - \hat{\beta}_i\|_1 > qM \sqrt{\frac{\log p}{T}} \right) \right] \rightarrow 0 \quad (17)$$

$$\sup_{\beta} \mathbb{E}_{\beta} [\mathbb{P}_{\cdot|D,\theta}(\hat{\beta} : \gamma(\hat{\beta}) > q(1+K))] \rightarrow 0 \quad (18)$$

The first limit is exactly the same as what has been proved in Rockova and George (2018), whereas the second limit can be proved with the same technique, but at a matrix level.

Theorem 6 (Rank-consistent posterior concentration)

Let q be independent of p and let p, T satisfy $\frac{\log p}{T} > \delta^2(qM)^{-2}$ eventually as $p, T \rightarrow \infty$.

$$\sup_{\beta} \mathbb{E}_{\beta} [\mathbb{P}_{\cdot|D,\theta}(\hat{\beta} : \tilde{r}(\hat{\beta}) \neq r)] \rightarrow 0$$

as $p, T \rightarrow \infty$

Proof. Let $B_j := \{\hat{\beta} : \gamma(\hat{\beta}) = j\}$ and $C := \{\hat{\beta} : \gamma(\hat{\beta}) > q(1+K)\}$. Observe

$$\sup_{\beta} \mathbb{E}_{\beta} [\mathbb{P}_{\cdot|D,\theta}(A)] \leq \sum_{j=0}^{q(1+K)} \sup_{\beta} \mathbb{E}_{\beta} [\mathbb{P}_{\cdot|D,\theta}(B_j \cap A)] + \sup_{\beta} \mathbb{E}_{\beta} [\mathbb{P}_{\cdot|D,\theta}(C \cap A)]$$

Now, it is clear from Equation 18 of lemma 5 that $\sup_{\beta} \mathbb{E}_{\beta} [\mathbb{P}_{\cdot|D,\theta}(C \cap A)] \rightarrow 0$ so it remains to prove $\sup_{\beta} \mathbb{P}_{\cdot|D,\theta}(B_j \cap A) \rightarrow 0$ for all $j \leq q(1+K)$.

1. When $j \leq q(1+K)$ and $j \neq q$, consider $\hat{\beta} \in B_j$. Observe that there exists i such that $\gamma_i(\hat{\beta}) \neq \|\beta_i\|_0$. Henceforth by construction, $\|\tilde{\beta}_i - \beta_i\|_1 > \delta$. Now, let set $I = \{i : \gamma_i(\hat{\beta}) \neq \|\beta_i\|_0\}$, where cardinality $|I| \leq q(2+K)$. Observe

$$\mathbb{P}_{\cdot|D,\theta}(B_j \cap A) \leq \mathbb{P}_{\cdot|D,\theta}(B_j) \leq q(2+K) \max_{i \in [p]} \mathbb{P}_{\cdot|D,\theta}(\{\tilde{\beta}_i : \|\tilde{\beta}_i - \beta_i\|_1 > \delta\}) \quad (19)$$

By lemma 5, we know $\forall i, \mathbb{P}_{\cdot|D,\theta}(\{\tilde{\beta}_i : \|\tilde{\beta}_i - \beta_i\|_1 > \delta\}) \rightarrow 0$ which completes the proof.

2. When $j = q$, reconsider $\hat{\beta} \in B_q \cap A$. As $\tilde{r}(\hat{\beta}) \neq r$, the set $I \neq \emptyset$. We can therefore bound, similarly to Equation 19, that

$$\mathbb{P}_{\cdot|D,\theta}(B_q \cap A) \leq q \max_{i \in I} \mathbb{P}_{\cdot|D,\theta}(\|\tilde{\beta}_i - \beta_i\|_1 > \delta) \rightarrow 0 \quad (20)$$

□

2.3 Algorithms

In general, the algorithms employ EM techniques to numerically approximate the estimators $(\hat{R}^{BE}, \hat{\sigma}^{BE}, \hat{\theta}^{ABE})$ as per Equation 11 and Equation 15. Write these as $(\hat{R}, \hat{\sigma}, \hat{\theta})$ and the approximated rank $\hat{r} := \text{rank}(\hat{R})$. The two algorithms differ by their approaches in λ_0 searching, in that algorithm 1 assumes the same value of $\lambda_{0,j} = \lambda_0 \forall j$ whereas algorithm 2 allows some degree of different increments of $\lambda_{0,j}$ and associated termination. Such difference is propagated through a uniform sampling on non-sparse coordinates.

2.3.1 Algorithm 1

As for notation, we use $e_{t,j}(k) = A_{t,j} - \beta_j(k)B_t = A_{t,j} - R(\cdot, j)(k)B_t$ to indicate the fitted j -th residual from the associated k -th iteration of the matrix estimate $R(k)$ for observations A_t, B_t . It is convenient to also use the following functions: p_θ^* and λ_θ^* , both of which are \mathbb{R} to $\mathbb{R}_{>0}$ mappings.

$$p_\theta^*(x) = \left(1 + \frac{\lambda_0(1-\theta)}{\lambda_1\theta} \times \exp(|x|(\lambda_1 - \lambda_0))\right)^{-1} \quad (21)$$

$$\lambda_\theta^*(x) = \lambda_0 + (\lambda_1 - \lambda_0)p_\theta^*(x) \quad (22)$$

In algorithm 1, we initialise a dummy estimate $\hat{r} = p$ and iteratively increase λ_0 per EM iteration. After each of the EM iterations, we re-estimate the rank. The iteration stops when \hat{r} gives the same rank for n_r times. This is done by the imposition of vector \tilde{r} .

2.3.2 Algorithm 2

In algorithm 2, we first use algorithm 1 to bring down the estimated rank to certain level of sparsity, here we state $\hat{r} < \frac{p}{2}$, but it may vary, certainly for large p to some level such as $\hat{r} < \sqrt{p}$ or $\hat{r} < \frac{T}{p}$. After bringing down the estimated rank, we implement an alternative approach where we sample $j \sim U(\{j : \hat{R}(\cdot, j) \neq \mathbf{0}_p\})$, i.e. a coordinate sampled uniformly from the set of non-zero coordinates of the estimated rows. We then implement the EM iterations on this row only, and update rank estimate accordingly. The technical change would also add on a different notion of p_θ, λ_θ due to the different $\lambda_{0,j}$ across coordinates. These are re-defined below:

$$p_\theta^*(x, j) = \left(1 + \frac{\lambda_{0,j}(1-\theta)}{\lambda_1\theta} \times \exp(|x|(\lambda_1 - \lambda_{0,j}))\right)^{-1} \quad (23)$$

$$\lambda_\theta^*(x, j) = \lambda_{0,j} + (\lambda_1 - \lambda_{0,j})p_\theta^*(x, j) \quad (24)$$

As the randomness (due to uniform sampling) exists, we may ensemble the results and provide a probabilistic output instead of a scalar estimate. For a set of seeds S , we may have estimates $\hat{r}(s)$ for $s \in S$. Statistics of these ranks, e.g. median and mean may offer insights into the approximate value of the estimated ranks.

Algorithm 1: Column-wise SSL through EM

Input: Data A, B ;
 Penalisation parameters $\lambda_0, \lambda_1, \Delta_\lambda$;
 Initialisers $\theta(0), \beta(0), \sigma_j^2(0)$;
 Halting controls K, ϵ_{cap}, n_r ;
 Parametric specifications for prior on θ_i : a_i, b_i
Output: Estimated ranks \hat{r} and matrix \hat{R}

- 1 Initialise estimation vector $\tilde{r} = (p + 1) \times \mathbf{1}_{n_r}$ and estimate $\hat{r} = p$.
- 2 Process data A, B such that all rows are centered at zero and all rows of B have variance T .
- 3 Iterative process on rank determination, by increase of λ_0 :
- 4 **while** $\tilde{r} \neq \hat{r} \times \mathbf{1}_{n_r}$ **do**
- 5 Update λ_0 with $\lambda_0 + \Delta_\lambda$
- 6 EM update on $(\beta, \theta, \sigma^2)$:
- 7 **for** $j \in [p]$ **do**
- 8 Initialise $\theta_j(0), \beta_j(0), \sigma_j^2(0)$, then
- 9 **for** $k \in [K]$ **do**
- 10
$$\beta_j(k) = \underset{\beta_j \in \mathbb{R}^p}{\operatorname{argmin}} \left\{ \sum_{t \in [T]} e_{t,j}(k)^2 + 2 \sum_{i \in [p]} \sigma_j^2(k-1) \lambda_{\theta_j(k-1)}^* (\beta_{i,j}(k-1)) |\beta_{i,j}(k)| \right\}$$
- $$\theta_j(k) = \frac{a - 1 + \sum_{i \in [p]} p_{\theta_j(k-1)}^* (\beta_{i,j}(k))}{a + b + p - 2}$$
- $$\sigma_j^2(k) = \frac{\sum_{t \in [T]} e_{t,j}(k)^2}{T - 2}$$
- $$\epsilon(k) = \|\beta_j(k) - \beta_j(k-1)\|_2$$
- if** $\epsilon(k) < \epsilon_{cap}$ **then**
- 11 | break the k for-loop
- 12 **end if**
- 13 **end for**
- 14 Collect $\hat{\beta}_j = \beta_j(k)$
- 15 **end for**
- 16 Collect $\hat{r} = \operatorname{rank} \left(\left[\hat{\beta}_1 | \dots | \hat{\beta}_p \right] \right)$
- 17 Replace $\tilde{r}_{1:(n_r-1)}$ with $\tilde{r}_{2:n_r}$ and replace \tilde{r}_{n_r} with \hat{r}
- 18 **end while**
- 19 Output estimated rank \hat{r} with the final matrix $\hat{R} = \left[\hat{\beta}_1 | \dots | \hat{\beta}_p \right]$

Algorithm 2: Column-wise SSL through EM with entry-wise λ_0 increment

Input: Data A, B ;
Penalisation parameters $\lambda_0 = (\lambda_{0,j})_{j \in [p]}, \lambda_1, \Delta_\lambda, \delta_\lambda$;
Initialisers $\theta(0), \hat{R}(0), \sigma^2(0)$;
Halting controls K, ϵ_{cap}, n_r ;
Parametric specifications for prior on θ_i : a_i, b_i
Seed for uniform sampling
Output: Estimated ranks \hat{r} , matrix \hat{R}

- 1 Process data A, B such that all rows are centered at zero and all rows of B have variance T .
- 2 Initialise $\hat{r} = p$
- 3 **while** $\hat{r} \geq \frac{p}{2}$ **do**
- 4 Use [algorithm 1](#) to update λ_0 with $\lambda_0 + \Delta_\lambda$ and EM update on $(\beta, \theta, \sigma^2)$
- 5 Collect $\hat{r}(\lambda_0) = \text{rank}(\hat{R}(\lambda_0))$
- 6 **end while**
- 7 Initialise estimation vector $\tilde{r} = (\hat{r} + 1) \times \mathbf{1}_{n_r}$
- 8 Initialise set $P = \{j : \hat{R}(\cdot, j) \neq \mathbf{0}_p\}$. Set seed for sampling.
- 9 Iterative process on rank determination, by increase of $\lambda_{0,j}$ for random j :
- 10 **while** $\tilde{r} \neq \hat{r} \times \mathbf{1}_{n_r}$ and $\hat{r} \neq 0$ **do**
- 11 Sample $j \sim U(P)$
- 12 Update $\lambda_{0,j}$ with $\lambda_{0,j} + \delta_\lambda |P|$
- 13 Initialise $\theta_j(0), \beta_j(0), \sigma_j^2(0)$ and EM update on $(\beta_j, \theta_j, \sigma_j^2)$ with the following steps:
- 14 **for** $k \in [K]$ **do**
- 15
$$\beta_j(k) = \underset{\beta_j \in \mathbb{R}^p}{\text{argmin}} \left\{ \sum_{t \in [T]} e_{t,j}(k)^2 + 2 \sum_{i \in [p]} \sigma_j^2(k-1) \lambda_{\theta_j(k-1)}^* (\beta_{i,j}(k-1), j) |\beta_{i,j}(k)| \right\}$$
$$\theta_j(k) = \frac{a - 1 + \sum_{i \in [p]} p_{\theta_j(k-1)}^* (\beta_{i,j}(k), j)}{a + b + p - 2}$$
$$\sigma_j^2(k) = \frac{\sum_{t \in [T]} e_{t,j}(k)^2}{T - 2}$$
$$\epsilon(k) = \|\beta_j(k) - \beta_j(k-1)\|_2$$
- 16 **if** $\epsilon(k) < \epsilon_{cap}$ **then**
 | break the k for-loop
- 17 **end if**
- 18 **end for**
- 19 Collect $\hat{\beta}_j = \beta_j(k)$
- 20 Obtain $\hat{R}(\lambda_0)$ by copying the previous $\hat{R}(\lambda_0)$ but replace the j -th column with $\hat{\beta}_j$.
- 21 Collect $\hat{r}(\lambda_0) = \text{rank}(\hat{R}(\lambda_0))$
- 22 **if** $\hat{\beta}_j = \mathbf{0}_p$ **then**
- 23 | Update P by $P \setminus \{j\}$
- 24 **end if**
- 25 Replace $\tilde{r}_{1:(n_r-1)}$ with $\tilde{r}_{2:n_r}$ and replace \tilde{r}_{n_r} with $\hat{r}(\lambda_0)$
- 26 **end while**
- 27 Output estimated rank \hat{r} with the final matrix \hat{R} and paths.

3 Simulation

3.1 Outline of Simulated Examples

The principle idea of the simulation task is to generate some big VAR(1) process and run algorithms 1 and 2 and collect the estimated ranks. The proposed VAR(1) process takes the following form

$$\Phi := (J(0, r) \oplus I_{(p-r)}) + \mathbf{1}_{r,r+1} \tag{25}$$

$$Y_t := \Phi Y_{t-1} + \varepsilon_t, \quad \varepsilon_t \sim N(0, \sigma^2 I_p) \quad \forall t \in [T] \tag{26}$$

with initialisation $Y_0 = 0$. If we write Equation 26 in the form of Equation 2, then

$$\Pi = \Phi - I_p = (J(0, r) - I_r) \oplus 0_{(p-r)} + \mathbf{1}_{r,r+1}$$

it is easy to see that $\text{rank}(\Pi) = r$.

For each tuple (p, r, T) , we generate $S = 100$ samples all satisfying $Y(s) \sim I(1)$ (checked by ADF test at 5% significance level), then proceed with the relevant algorithms to collect ranks. As algorithm 2 gives a probabilistic inference on the rank instead of a numerical estimate, we instead enquire algorithm 2 100 times per sample, and take the mean as the estimated rank. The general algorithm is drawn below.

Algorithm 3: General algorithm for simulated examples

Input: T, p, r ; and number of successfully simulated samples $S = 100$

Output: Estimated ranks $\hat{r}(i)$ for $i \in [S]$

- 1 Initialise `successful_seed` = 0 and seed $s = 0$
 - 2 Create Φ
 - 3 **while** `successful_seed` $\leq S$ **do**
 - 4 Generate $\varepsilon_t(s) \sim N(0, \sigma^2 I_p)$ in accordance with the seed s
 - 5 Compute the corresponding $Y_t(s), t \in [T]$
 - 6 Use standard ADF test to test for $Y(s) \sim I(1)$. If failed at 5% significance level, we reject the sample and re-draw by replacing s by $s + 1$.
 - 7 Run the appropriate algorithm and report $\hat{r}(s)$, replce `successful_seed` by `successful_seed + 1`.
 - 8 **end while**
-

3.2 Summary of Results

3.2.1 Algorithm 1

For algorithm 1, we simulate two sets of regime. In the first regime, we consider $p = 10, T = 100$, and we scan the cases for $r \in [5]$. In the second regime, we consider $p = 30, T = 300$, and we scan the cases for $r \in [5]$.

Figure 1 shows the percentage correct obtained under these regimes, plotted over the true r . For instance, when $r = 0$, algorithm 1 detects 100% correct in terms of $\hat{r} = 0$ for both $p = 10$ and $p = 30$, whereas when $r = 5$, the algorithm detects only 65% correct in terms of $\hat{r} = 5$ for $p = 30$, and 86% correct for $p = 10$.

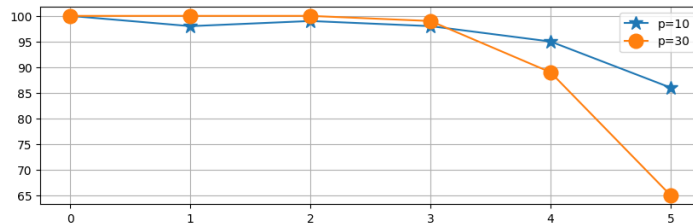


Figure 1: Percentage Correct (Accuracy of rank estimation)

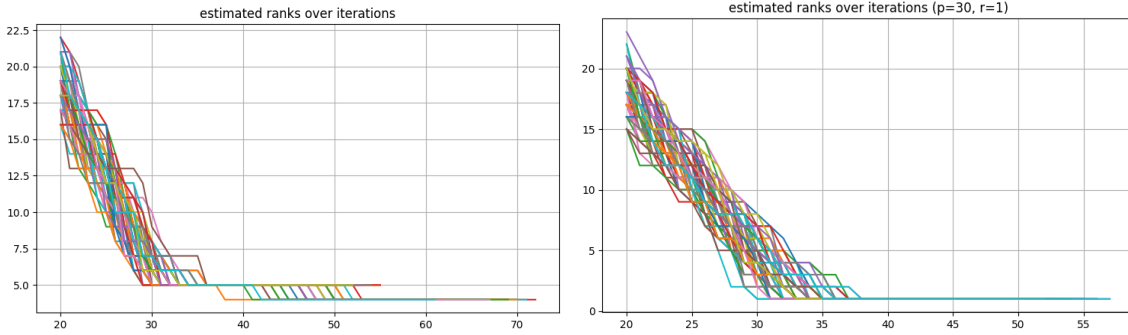


Figure 2: Estimated ranks over iterations

Figure 2 investigates potential issues arising from higher-rank under-penalisation. Particularly, we focus on the case of $p = 30, r = 5$ against the case of $p = 30, r = 1$. The latter got 100% correct in accuracy, whereas the earlier performs poorly. As shown on the iteration graph on the left, while many terminates when $\hat{r} = 5$, a good portion dropped to $\hat{r} = 4$ and terminated there. This means the iterative increase of λ_0 has over-penalised the matrix, leading to an over-sparsified estimation of some rows — leading to an under-estimation of ranks.

The promising result is on the right — under more sparsified regimes, we can see all ranks converging to 1 and terminating there, which means no over-peanlisation by SSL specifications.

3.2.2 Algorithm 2

For algorithm 2, we demonstrate the advancement from algorithm 1 in the following two ways: better performance (with reasons) under the high-dimensional ($p = 30, T = 300$) regime, and the ability to handle even higher-dimensional ($p = 100, T = 500$) regime. In both regimes, we experiment $r \in \{1, 5\}$.

An overall summary for approximate percentage correct is illustrated in Table 1. The first column specifies the regime set-up and algorithm in comparison, whereas the second and third column give the definition of percentage correct. As indicated in the algorithms, the algorithm 2 only provide probabilistic estimation instead of scalar estimation of the ranks. Here, we take the average of all 100 different randomisation — therefore many estimations may not be an integer, and hence the need to draw some notion of approximation. The second column of the table indicates percentage correct of falling into an estimation between $r - \frac{p}{100}$ and $r + \frac{p}{100}$. For instance, when $p = 30, r = 5$, algorithm 1 gives 65 estimations correctly within the 4.7-5.3 range, whereas algorithm 2 gives 94 estimations correctly within the same range. The algorithm 2 further estimate all scenarios correctly when we relax the range into between $r - \frac{p}{50}$ and $r + \frac{p}{50}$.

p, r	$r \pm \frac{p}{100}$	$r \pm \frac{p}{50}$
$p = 30, r = 1$ (algorithms 1 and 2)	100	100
$p = 30, r = 5$ (algorithm 1)	65	65
$p = 30, r = 5$ (algorithm 2)	94	100
$p = 100, r = 1$ (algorithm 2)	84	100
$p = 100, r = 5$ (algorithm 2)	100	100

Table 1: Approximate percentage correct by definitions

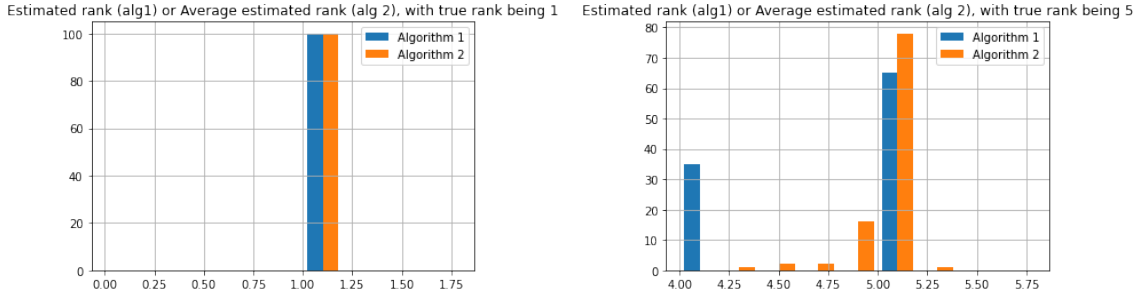


Figure 3: Histograms of estimated ranks over samples for $p = 30, T = 300$

As an additional comparison between algorithm 1 and 2, we show the histogram of estimated \hat{r} across the 100 samples in Figure 3. The blue histograms indicate estimations given by algorithm 1 — 100% correctly in the case of $r = 1$ whereas having a 35% incorrect estimation ($\hat{r} = 4$) when $r = 5$. Algorithm 2 picks up the incorrectness in a more probabilistic manner — hence the average being more concentrated around 5, resulting in more accurate results in Table 1.

As an interactive showcase between the two algorithms, we draw one sample in the case of $r = 5$ and $r = 1$ and show the iteration paths from both algorithms in Figure 4. Algorithm 1 is highlighted in red. As per previous narratives, from the top graph, we can see the drop into $\hat{r} = 4$ which concludes its fate into over-penalisation. For algorithm 2, the start of the iteration trajectories are exactly the same as algorithm 1 up to the iteration where $\hat{r} = 12$. It then starts the randomised paths, resulting in potentially different pathways to draw down to, eventually, the level of $\hat{r} = 5$ or 6. Most of them eventually terminated at $\hat{r} = 5$. A similar story may be seen for the lower graph where termination occurred mostly at $\hat{r} = 1$.

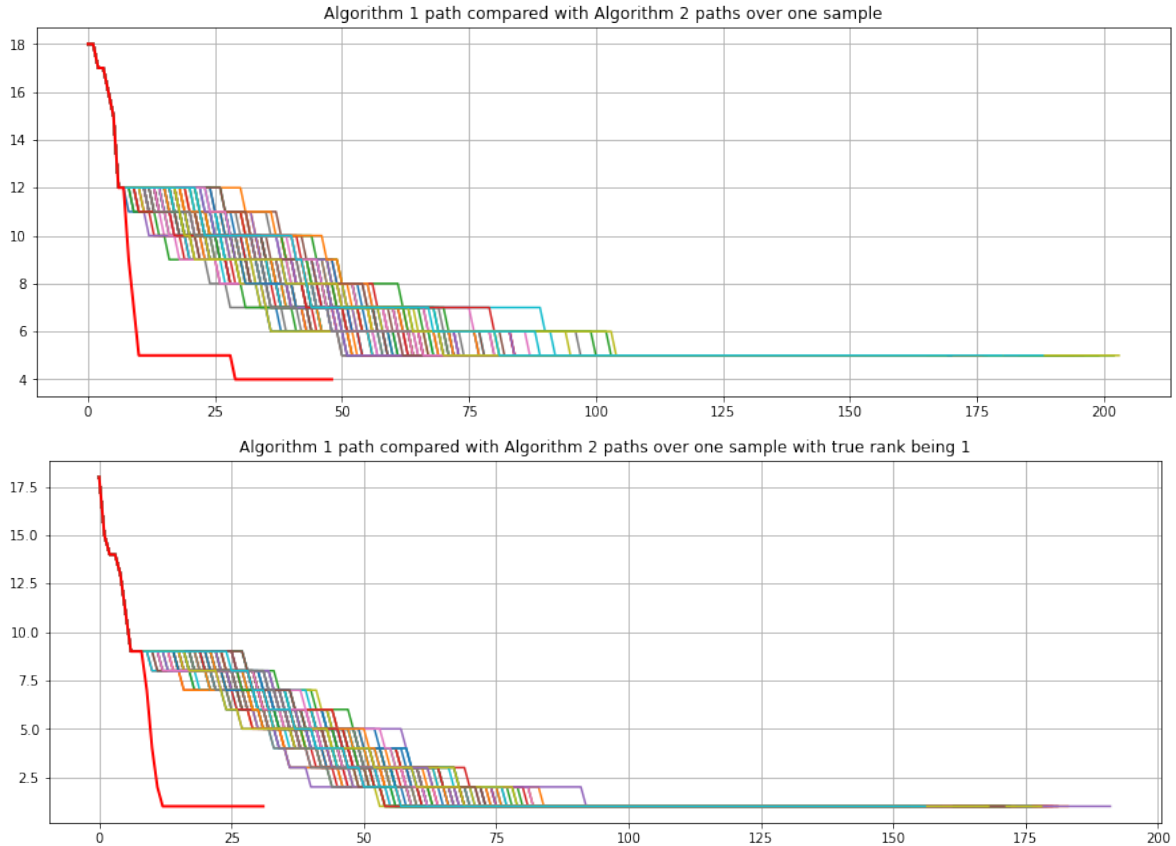


Figure 4: Estimated ranks over iterations

The cases where $p = 100, T = 500$ are presented in [Figure 5](#) for histograms and [Figure 6](#) for one sample path. As can be seen, there are significant concentration at around the true rank for both cases — more significantly so for $r = 5$. This corroborates the summative statistics provided back in [Table 1](#).

In [Figure 6](#), we show an example of the case where $r = 5$ and also in comparison with the red line (algorithm 1) which fails to estimate the true rank by under-estimating it to $\hat{r} = 0$. In this example, mean estimation from algorithm 2 is 4.91 with median as 5.0.

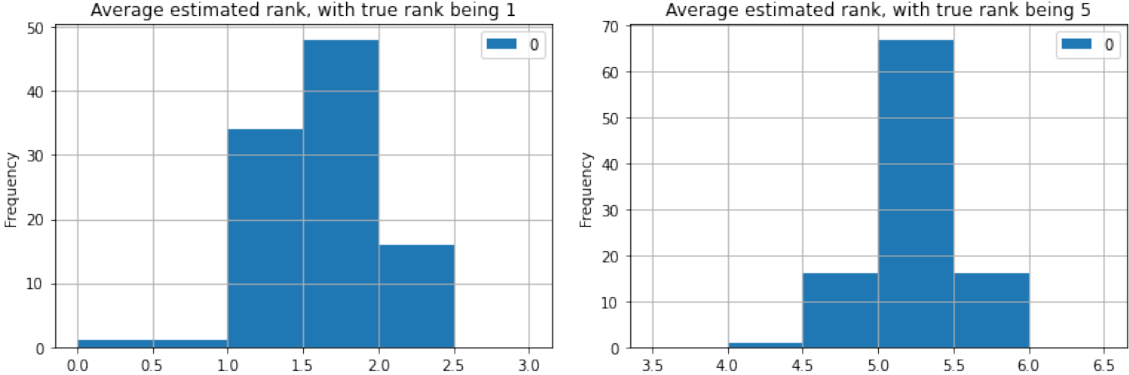


Figure 5: Histograms of estimated ranks over samples for $p = 100, T = 500$

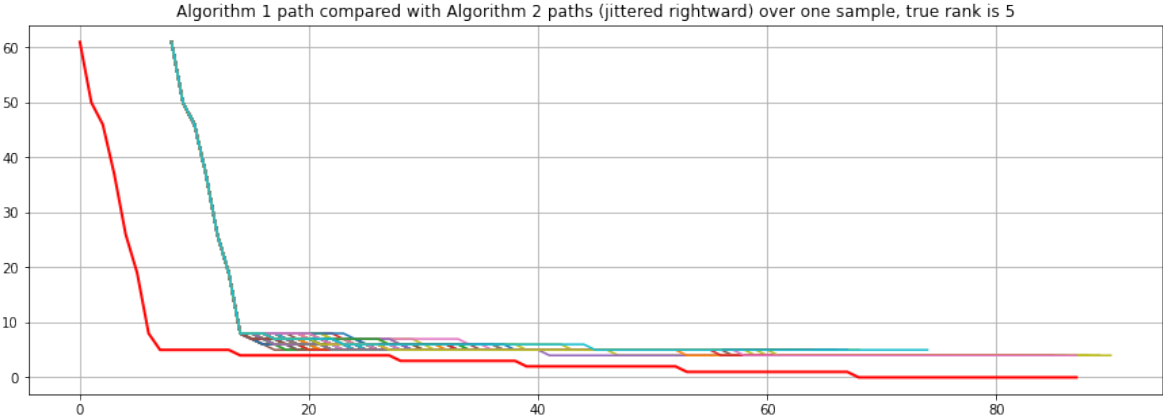


Figure 6: Estimated ranks over iterations

4 Empirical application to stable portfolio

The principle idea of this empirical application is to find a collection of unitary portfolio allocations $(\alpha_i)_i$ such that each portfolio α_i of assets has minimum variance — hence denoted stable portfolio. By using cointegration analysis, it is expected that such minimum variance could persist not only in the training dataset, but also in the unseen testing dataset proceeding from the training.

4.1 Portfolio construction

After obtaining \hat{R} and \hat{r} , the key idea is to use \hat{R} to reconstruct $\hat{\Pi}$ and hence obtain \hat{r} number of co-integrating vectors. These vectors, upon normalisation, yield exactly a portfolio which we may analyse, assuming a single dollar and zero-cost implementation on a long-short portfolio on the relevant universe of assets.

Let $\hat{\Pi}$ be the recovered Π where $\hat{\Pi} = (\tilde{S}\hat{R})^\top$. Let $\hat{\Pi}_i$ be a non-zero row vector of $\hat{\Pi}$. A portfolio is therefore constructed with value at time t being $\alpha_i Y_t$, where $\alpha_i := \frac{\hat{\Pi}_i}{\|\hat{\Pi}_i\|_1}$.

4.2 Data and Preparation

We obtain daily stock prices of all individual stocks in SPX 500 as of end of September 2023. The price time series start from January 2022 to September 2023 (this gives 374 observations, though it also means $T < p$), and we use from the January 2022 to June 2023 for in-sample training, and July to September 2023 for out-of-sample testing. We use ADF test to check for I(1) non-stationarity. Out of the 500 stocks, 405 stocks are I(1). We are henceforth in a regime of $T = 374$ and $p = 405$.

The only pre-processing to be done is to compute for cumulative return in relation to the start of the dataset, that is, to have $\frac{Y_{t,j}}{Y_{1,j}}$ as the time series for investigation.

4.3 Main Results

We run 100 repetitions of algorithm 2 to show various portfolio results, and then illustrate a number of implied portfolios from one of the results in algorithm 2 to demonstrate the performance and insights.

4.3.1 Inference on estimated rank in algorithm 2

Because of the probabilistic nature of [algorithm 2](#), we are able to produce slightly different $\hat{\Pi}$ upon different seeds for the uniform distribution, and hence potentially different \hat{r} owe to different timings of termination of algorithms and different compositions of λ_0 vector. For a set of seeds S^{seed} , we are able to obtain $\{\hat{r}(s) : s \in S^{seed}\}$ which serves as an inference on \hat{r} .

In [Figure 7](#), we plot the estimated ranks over iterations on the left, and the histogram of $\{\hat{r}(s) : s \in S\}$ on the right. An average rank of around 1.6 is being estimated.

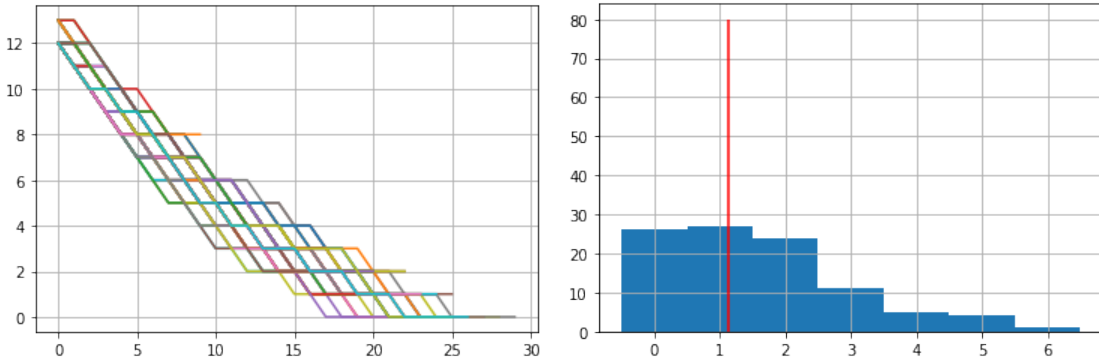


Figure 7: Path of estimated ranks over stages of $\lambda_{0,j}$ increments (left); Histogram of estimated ranks over different seeds (right)

4.3.2 General training and testing performance

For each seed $s \in S^{seed}$, as long as $\hat{r}(s) > 0$, we have $\hat{r}(s)$ amount of portfolios implied from the cointegration relationships. We evaluate the stability of the portfolio by measuring the standard deviation of daily returns (in percentage), commonly known as ‘portfolio volatility’ in financial literature.

In [Figure 8](#), we plot histograms of the training and testing volatilities of all such portfolios over all seeds. The values are much lower than the underlining index in both training and testing (see [Table 2](#) for the index and equally-weighted portfolio volatility in the corresponding periods).

This has demonstrated the ability of cointegrated portfolio to reduce variance by a huge portion.

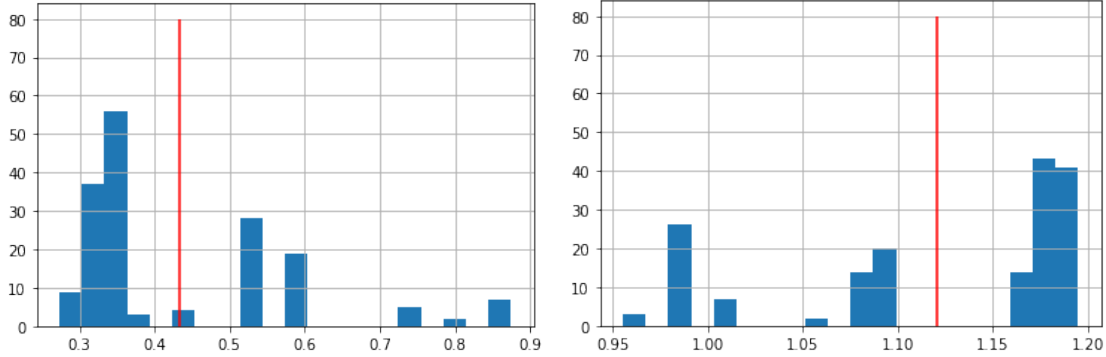


Figure 8: Portfolio volatility in training and testing over different seeds

4.3.3 Example portfolio performance and insight

Portfolio	Training	Testing
SPY Index	18.4	10.8
Equally Weighted	18.2	10.8
Cointegration 1	0.4	1.1
Cointegration 2	0.3	1.1
Cointegration 3	0.9	1.0

Table 2: Training and Testing period standard deviation of daily returns (in percentage)

We select a particular seed where $\hat{r}(s) = 3$ and illustrate the results from the corresponding 3 portfolios. In [Table 2](#), we report the portfolio volatilities of the three portfolios — there is a massive decrease of volatilities from the underlining index / equally weighted portfolio. We plot the cumulative returns in [Figure 9](#) for training period (upper) and testing period (lower), and there is a clear and meaningful stability in contrast to the index and equally weighted portfolio.

As to the portfolio insight, we investigate the top 25 stocks’ weighting of each of the 3 portfolios in the first three graphs of [Figure 10](#). These weights are also plotted against the SPY index and horizontal lines indicating the equally-weighted weights. We can see that though some handful similarities, the main long-short focus of the portfolios differ significantly to the SPY index. An alternative graph at the bottom illustrates the weighting of the top 25 stocks from SPY in the respective portfolios. This also supports the insight that the focus of the cointegrated portfolios has not been on the highly capitalised stocks, compared to SPY.

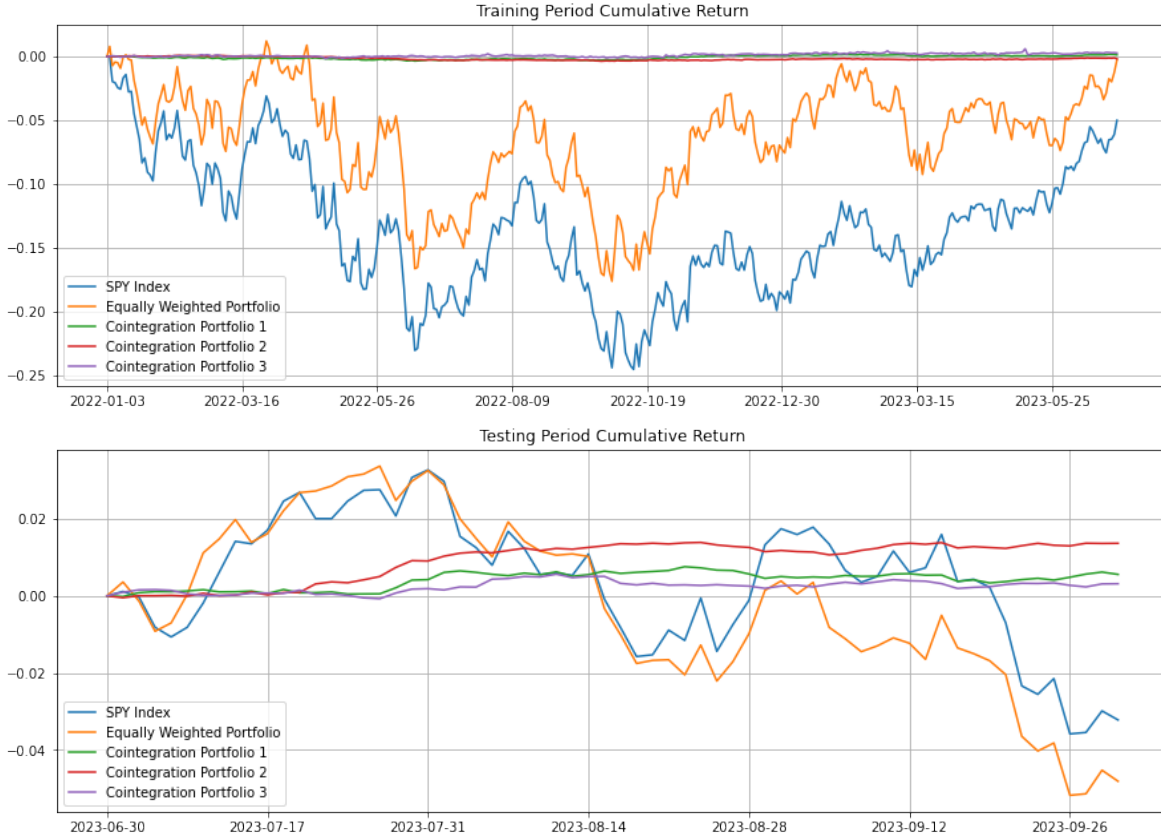


Figure 9: Cumulative return plots.

5 Conclusion

5.1 Discussions

Though algorithm 2 has the drawbacks of requiring some moderate amount of sparsity assumption, it significantly outperforms algorithm 1 by halting the λ_0 increment appropriately. Moreover, algorithm 2 enables some probabilistic inference on the estimation \hat{r} , in the sense that $j \sim U(P)$, i.e. $\{\lambda_{0,j} : j \in [P]\}$ being attributed on some randomised size each time the iteration goes. This adds a further Bayesian layer in the modelling hierarchy, and gives an interpretable histogram as one designs the number of repetitions to run the algorithm.

In terms of the higher dimensional investigation, we reached to $p = 100, T = 500$ in simulation and $p = 405, T = 374$ in empirical application. It is worth appreciating that algorithm 2 scales down computing time for large p , as it only requires one β_j update per iteration due to the sampled index, instead of mass update of the whole matrix as per algorithm 1. A compute-time relevant adjustment is also available at line 3 — in essence, one may wish to tune down the sparsity assumption (such as subject to an identifiability constraint $pr < T$) and therefore increase Δ_λ to achieve faster runtime. This is not possible to be done in algorithm 1.

A number of future works are thought to be helpful based on the current investigation: we may investigate a even larger number of features, either in the numerical sense (e.g. $p > 1000$) or in the asymptotic sense of $p = O(T)$. The asymptotic inference may also be drawn towards approximate correctness, such as $\hat{r}/r \rightarrow 1$ with more generic limits such as $q, r \rightarrow \infty$. This then leads to space for investigating even higher dimensional cointegration in applied fields, such as portfolio construction and adjustments.

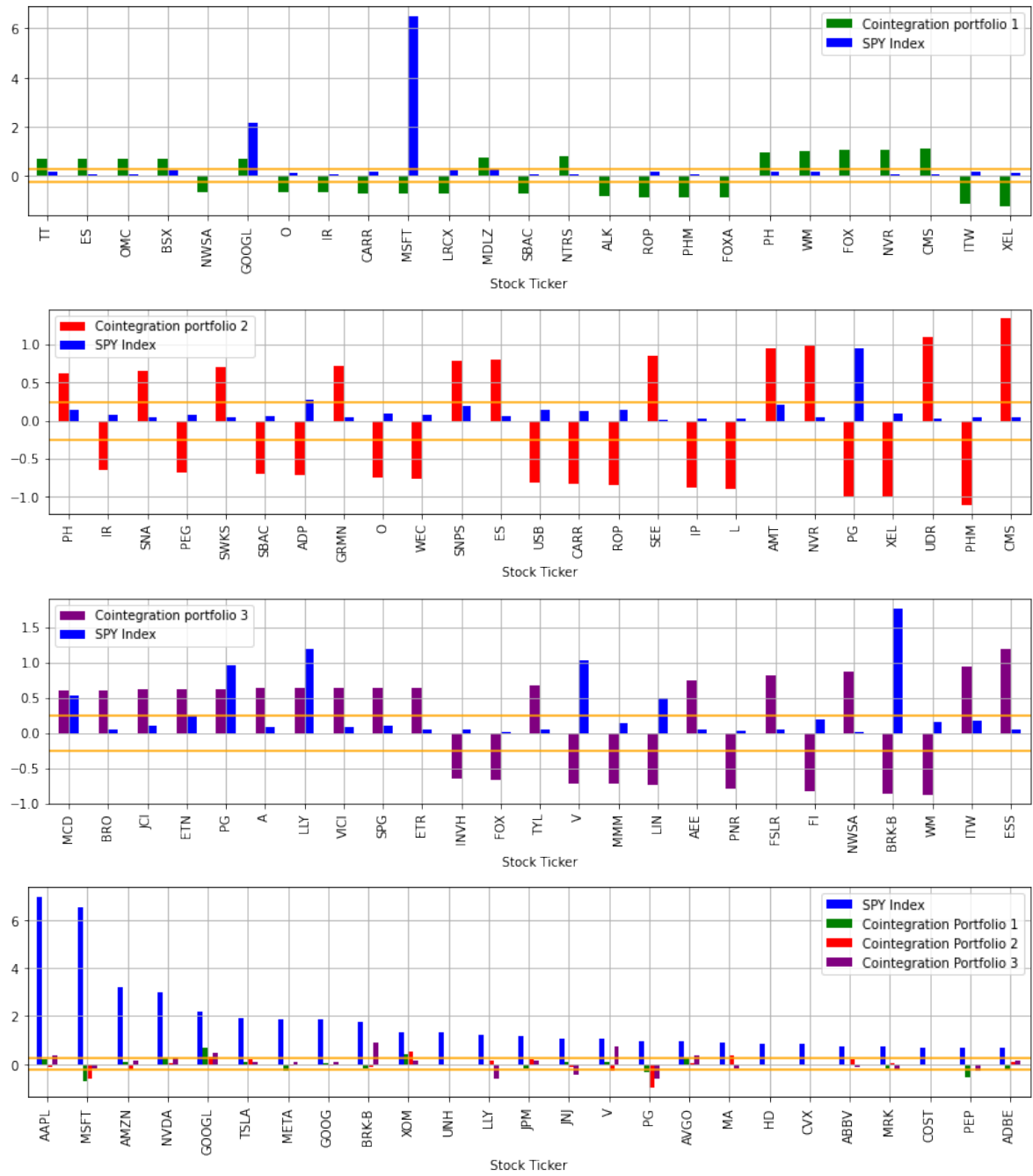


Figure 10: Portfolio Insights.

5.2 Contribution

There are mainly three forces of contributions being brought from this paper. First, similar to Liang and Schienle (2019) and Chen and Schienle (2022), we extend the "Traditional identifiability constraint" from $p^2 < T$ to $pr \leq T$, in the sense that through penalisation, one does not necessarily need more observations than unknowns to estimate the cointegration matrix and thereafter the number of cointegration relationships in the system. Instead, through SSL, we proposed nuanced methodologies to estimate r and also showed some level of asymptotic convergence in a Bayesian setting.

Secondly, we used various simulation regimes to test our proposed algorithms. This furthers the SSL executions from optimally finding a p dimensional sparse vector to finding a $p \times p$ dimensional sparse matrix and determining its true rank. Particularly, the termination of λ_0 increment varies substantially from existing Bayesian literature, as we quantify further the termination criteria instead of a generic guidance on convergence-termination. This contributes to the implementation of SSL and furthered the agenda to use Bayesian modelling as a "pragmatic frequentist" on penalisation.

Lastly, the application to portfolio construction contributes to the relevant financial literature. Our algorithms yield various independent and insightful portfolios that yield low volatilities, as cointegration theory would presume, which invite further studies on topics such as efficient hedging and portfolio construction.

A Technical appendix

A.1 Data processing

Recall that our data, in matrix form, can be written as $A = [\Delta Y_1, \dots, \Delta Y_T] = [A_1, \dots, A_T] \in \mathbb{R}^{p \times T}$ and $B = [\tilde{S}^T Y_0, \dots, \tilde{S}^T Y_{T-1}] = [B_1, \dots, B_T] \in \mathbb{R}^{p \times T}$ where $A_t, B_t \in \mathbb{R}^{p \times 1}$. The data processing tasks concerns transformation from A to \tilde{A} and B to \tilde{B} such that

- \tilde{A} is centralised, i.e. $\sum_{t \in [T]} \tilde{A}_t = 0_p$. This can be done by

$$\tilde{A}_t = A_t - \frac{\sum_{t \in [T]} A_t}{T} \quad (27)$$

- \tilde{B} is centralised and with \sqrt{T} of standard deviation each row. This can be done by

$$\tilde{B}_{t,j} = \sqrt{T} \frac{B_{t,j} - \mu_{B,j}}{\sigma_{B,j}} \text{ where } \mu_{B,j} = \frac{\sum_{t \in [T]} B_{t,j}}{T} \text{ and } \sigma_{B,j} = \sqrt{\sum_{t \in [T]} \frac{(B_{t,j} - \mu_{B,j})^2}{T}} \quad (28)$$

References

- Bai, Ray, Veronika Rockova, and Edward I George (2021). “Spike-and-slab meets lasso: A review of the spike-and-slab lasso”. In: *Handbook of Bayesian Variable Selection*, pp. 81–108.
- Chen, Shi and Melanie Schienle (2022). “Large Spillover Networks of Nonstationary Systems”. In: *Journal of Business & Economic Statistics*, pp. 1–37. DOI: [10.1080/07350015.2022.2099870](https://doi.org/10.1080/07350015.2022.2099870).
- Engle, Robert F. and C. W. J. Granger (1987). “Co-Integration and Error Correction: Representation, Estimation, and Testing”. In: *Econometrica* 55.2, pp. 251–276.
- Johansen, Søren (1991). “Estimation and Hypothesis Testing of Cointegration Vectors in Gaussian Vector Autoregressive Models”. In: *Econometrica* 59.6, pp. 1551–1580.
- Liang, Chong and Melanie Schienle (2019). “Determination of vector error correction models in high dimensions”. In: *Journal of econometrics* 208.2, pp. 418–441.
- Rockova, Veronika (2018). “Bayesian estimation of sparse signals with a continuous spike-and-slab prior”. In: *The Annals of Statistics* 46.1, pp. 401–437. DOI: [10.1214/17-AOS1554](https://doi.org/10.1214/17-AOS1554).
- Rockova, Veronika and Edward I. George (2016). “Bayesian penalty mixing: The case of a non-separable penalty”. In: *Statistical Analysis for High-Dimensional Data*. Springer, pp. 233–254.
- (2018). “The Spike-and-Slab LASSO”. In: *Journal of the American Statistical Association* 113.521, pp. 431–444.